A metal-polymer composite with unusual properties

A metal-polymer composite with unusual properties.

D. Bloor [1, 2], K. Donnelly [1,a], P. J. Hands [1], P. Laughlin [2], and D. Lussey.[2]

[1]Department of Physics, University of Durham, South Road, Durham, DH1 3LE

and

[2]Peratech Ltd., G3 Morton Park Way, Darlington, Co. Durham, DL1 4PJ.

Abstract.

Electrically conductive composites that contain conductive filler dispersed in an insulating polymer matrix are usually prepared by the vigorous mixing of the components. This affects the structure of the filler particles and thereby the properties of the composite. It is shown that by careful mixing nano-scale features on the surface of the filler particles can be retained. The fillers used possess sharp surface protrusions similar to the tips used in scanning tunnelling microscopy. The electric field strength at these tips is very large and results in field assisted (Fowler-Nordheim) tunnelling. In addition the polymer matrix intimately coats the filler particles and the particles do not come into direct physical contact. This prevents the formation of chains of filler particles in close contact as the filler content increases. In consequence the composite has an extremely high resistance even at filler loadings above the expected percolation threshold. The retention of filler particle morphology and the presence of an insulating polymer layer between them endow the composite with a number of unusual properties. These are presented here together with appropriate physical models.

[a] Present address: Microengineering and Biomaterials Group, Faculty of Engineering and Physical Sciences, University of Dundee, Dundee, DD1 4HN.

1. Introduction

The properties of composites comprising electrically conductive particles dispersed in an insulating polymer matrix have been studied for over 50 years.[1, 2, 3, 4, 5] Carbon and metal powders, e.g. Ni, Cu, Ag, Al and Fe, have all been used as fillers. Carbons utilised include carbon nanotubes, carbon fibre, graphite, pyrolytic carbons and carbon blacks, the latter having large variations in purity and morphology. The metal powders offer well-defined morphology and a higher intrinsic conductivity than carbon black. In general, at low filler content the conductive particles are well separated and the composite is insulating with an electrical conductivity only slightly higher than that of the polymer. Initially the conductivity increases slowly with filler concentration, but then rises rapidly over a narrow concentration range to give a high conductivity with only a weak dependence on further increase in filler concentration.

Percolation theory is commonly used to describe the behaviour in the region of rapidly varying conductivity.[4, 5] The conductivity rises at the percolation threshold as the conductive particles begin to aggregate to produce chains of particles in intimate contact, providing conductive paths spanning the sample. The conductivity increases rapidly as more percolation paths form until saturation is approached when the conductivity rises slowly to its maximum value. This model fails below the percolation threshold where it predicts that the composite is an insulator. Effective medium theories have been developed that provide a good description of the evolution of the conductivity across the full range of filler concentrations.[4, 6] The concentration of filler particles at the percolation threshold is sensitive to the shape of the particles. Values of the volume fraction of filler at the percolation threshold are observed to range from < 1% for needle-like particles to > 10% for spherical particles. Low percolation thresholds occur in anisotropic composites when chains of aligned filler particles are produced during processing, usually by the application of electric or magnetic fields.[4] Anomalous behaviour is observed with some carbon blacks due to agglomeration of the individual particles.[7, 8]

Despite the long history of experimental and theoretical studies of conductive composites, there is an on-going discussion about the relative importance of different

conduction mechanisms.[9, 10] While examples are known of systems where the filler particles are in direct physical contact,[5] in general in the percolation regime the conducting chains will contain gaps across which electrons can tunnel. The thermal fluctuation of the inter-particle tunnelling barrier has been used to explain the behaviour of the conduction at low temperature. [11, 12, 13] It has also been demonstrated that in the percolation regime any external influence that affects particle separation, and hence electron tunnelling, will give rise to a large change in resistance.[14, 15] The piezoresistance, i.e. the change in resistance of the composite under external forces, has been analysed using the percolation model and, for fibrous fillers, in terms of fibre reorientation.[14-16] Tunnelling has also been implicated in the rapid increase in resistance with temperature, the positive temperature coefficient (PTC), which occurs in most composites.[3, 4] In carbon black-polyethylene composites this has been attributed to the fact that the carbon black particles are excluded from crystalline regions and accumulate in the amorphous regions. An increase in the amorphous polymer fraction close to the melting point allows filler particles to move apart, creating wider tunnelling barriers and breaking up percolative chains. This model does not explain a number of results, notably the occurrence of a PTC effect in composites with amorphous polymer matrices.[17] This has been attributed to the interplay of thermal expansion and internal stress giving rise to significant changes in inter-particle separation, thereby affecting tunnelling barriers and the conductivity.

While tunnelling is important in determining the properties of composites, a number of other mechanisms that could play a role in conduction have been considered. Electric field induced emission was once considered to be important,[18] particularly at high fields.[19] Schottky emission, Poole-Frenkel conduction and space charge limitation of conduction with Fowler-Nordheim tunnelling via traps have also been used to model conduction in composites.[20] During the preparation of metal-polymer composites metal ions may be dispersed in the polymer matrix, and mobile ionic species,[13] and possibly electrochemistry, may contribute to conductivity. Given the complexity of conductive composites the possibility of the occurrence of these conduction mechanisms should not be ignored in the analysis of experimental data.

We report here the properties of a new type of composite, QTC™, produced by Peratech Ltd. The company has developed a process by which metal particles with sharp projections on the surface are wetted perfectly by the host polymer.[21] These composites display a range of unique properties not observed in other composites. The composites remain insulating at filler to polymer loading of 4 to 6:1 by weight, which is normally sufficient to produce a material either in or above the percolation regime. This results in a large piezoresistive effect, as the resistance of the composites is extremely sensitive to deformation. Under modest compression the sample resistance can fall from circa 10^{12}-10^{13} ohm to less than 1 ohm, an exceptionally large dynamic range for a property of a solid material at room temperature. When compressed into the low resistance state the composite can carry large currents without observable damage. Furthermore, the resistance also falls reversibly when the material is stretched, bent or twisted. This behaviour is unlike that of conventional conductive composites for which the resistance increases on extension.[22, 23] Similarly, the highly non-linear current-voltage characteristics of deformed samples, with negative resistance regimes, are unlike those reported for other composites.[24] A description of the properties of these composites and of possible physical mechanisms underlying them is presented below.

2. Experiment.

Samples of composite comprising nickel powders in an elastomer matrix were prepared at Peratech Ltd by a patented process,[21] which involves the careful mixing of nickel powders and liquid monomers. Nickel powders were obtained from Inco Ltd. Those used in this work were type 123, manufacturer's quoted particle size distribution measured by Fisher sub-sieve sizer from 3.5 to 4.5 micron, and type 287, quoted particle size in the range 2.6-3.3 μm. However, electron microscope observations revealed a somewhat larger size range extending from below 1 μm to above 10 μm, see §3.2 below. The powders were used as supplied and incorporated at loadings of metal to polymer of between 4:1 and 6:1 by weight (400 to 600 phr) in the composite. The monomers used were either silicone or urethane based. Silicones included Alphasil 2000 (Alphas Industries Ltd.), Silcoset 153 (Ambersil Ltd.), Silastic T4 (Dow Corning) and RTV6166 (GE Silicones) and the urethane was F42 (Techsil

Ltd.). The mixture was prepared as described in ref. 21, calendared and the monomer polymerised following the manufacturer's instructions, to produce flexible sheets of controlled thickness. Samples were cut from these sheets with either a sharp knife or a hole punch. Samples for scanning and transmission electron microscopy were prepared by freeze fracturing and microtoming, respectively. These were examined in a Jeol JSM IC848 SEM and Jeol JEM 200CX TEM. The composition of the samples used in these studies is given in the figure captions.

The resistance of undeformed samples was measured by the four-point probe method, with four in-line conductive paint contacts, using a Keithley Model 610C electrometer in current mode and between the inner contacts with the electrometer set to measure resistance. The piezoresistance was measured for compressed, stretched and bent samples. A variety of metals were used to make electrical contact to the composites, these included aluminium, nickel, gold, copper, chromium, brass and steel. No significant dependence of the results on electrode material could be discerned and low resistances, of the order of a few ohms or less, were observed for deformed samples regardless of electrode material. Cylindrical samples, 5.5 mm in diameter and 2 mm thick, with nickel electrodes in contact with the upper and lower surfaces, were subjected to uniaxial compression in a Lloyd Model LX100 mechanical tester. Sample resistance was measured with a purpose-built, constant current source, providing currents of between 1 μA and 10 mA, and an analogue to digital converter (Pico ADC-100) connected to a PC; data was collected and displayed with Picoscope™ software. The range of resistance values that could be measured at a given current was less than the total change in resistance of the composite so that several current settings were used. When the current was reset the compression was reduced so that the measurement ranges overlapped. At higher compression the viscoelastic behaviour of the composite resulted in an offset of the values in the region of overlap, this is seen in the results presented below.

A QTC™ sheet was stretched on an optical slide with micrometer adjustment. The opposite edges of the sample were held in contact with gold electrodes by clamps the separation of which was set by the micrometer. The undeformed, freestanding portion of the sample had dimensions $20 \times 20 \times 1$ mm. The sample resistance was measured

between the clamps with a Beckman Circuitmate DM25XL digital multimeter with an upper measurement limit of 200 MΩ. As the sample was stretched the lateral dimensions of the central portion of the sample were visibly reduced, however, the width of the clamped edges was unaltered. Samples, 1 mm thick, were bent over cylinders of different radii. The resistance was measured parallel to the bending axis. Two chromium plated probes, separated by 10 mm along the line of minimum radius, were brought in to light contact with the sample. The resistance was measured with the Beckman multimeter. Radii were taken as the sum of the cylinder radius and the sample thickness. As the sample thickness is reduced for cylinders with radii below 2 mm this overestimates the smallest radii, an increased experimental error is introduced to allow for this.

Current-voltage curves were recorded for cylindrical samples, typically 5.5 mm diameter and 2 mm thick, compressed in a micrometer-adjusted clamp. The stainless steel jaws of the clamp were brought into direct physical contact with the QTC. Alternatively foils of aluminium, copper and gold were inserted between the jaws and the QTC sample. As noted above the use of different contact materials had no noticeable effect on the measurements. Pressure was monitored with a 940-241E Mitutoyo force gauge with digital output. A Keithley Model 2420 digital high voltage SourceMeter™ interfaced to a PC was used to collect data. Voltage sweeps and data collection were controlled by a Labview™ programme.

All experiments were carried out at room temperature.

3. Results and discussion.

3.1 Response to external forces

The sheets of QTC™ composite used in this study are flexible and dark grey in colour. The flexibility depends on the grade of elastomer used as matrix, the filler loading and the sheet thickness. Thin sheets with low filler loading are the most flexible. When the sheets are deformed the resistance falls for all deformations, i.e. compression, elongation, bending and twisting. For rigid materials of uniform cross

section that have only small dimensional changes under an applied force it is possible to separate the effects of the changes in sample dimension and the resistivity of the material.[25] QTC™ is a soft deformable material, even at the highest filler loading. The changes in dimensions and shape under external forces are considerable. At the highest deformations the samples are clearly not homogenous. Inevitably quantities such as the resistivity, electric field and current density will not be constant throughout the sample. Therefore, we present our data in terms of the resistance for samples of defined composition and initial dimensions, and the measured compression, extension and bending. An estimate for the resistivity of undeformed samples is ~ 10^{11} Ωm while that of the most highly compressed samples is ~10^{-3} Ωm. Typical data for compressed, stretched and bent samples are shown in Figs. 1-3.

Results for a compressed sample is shown in Fig. 1. The resistance of the uncompressed sample was too large to be measured, the instrumental limit being 10 Mohm. However, the resistance of an uncompressed sample of a similar composite was measured to be 10^{12} ohm and it is reasonable to assume that the initial resistance was in this instance, allowing for the different sample dimensions, ca. 10^{10} Ω. The lowest resistances observed for compressed samples ~0.01 ohm. The variation in resistance under compression is reproducible providing that the measuring current is kept small, effects due to charge storage in the composite at higher current levels are described in section 3.3. Samples have been reproducibly cycled between the insulating and conductive states for one million cycles. During the measurements shown in Fig. 1 the output of the current source was switched as described in §2 and some offsets occur for compression >17%. The circle plotted round each data point indicates the measurement error. Within the error the resistance depends exponentially on compression up to ca. 21% compression beyond which a different dependence is observed. Joule heating of the sample is insufficient to account for the deviation at high compression as the electrodes provide a large thermal sink. Sample temperature was measured with an IR thermometer for the clamp used for current voltage characteristics, which is a similar thermal environment, and the maximum temperature increase for both sample and electrodes was found to be a few degrees Centigrade under similar electrical conditions. A possible cause of this deviation is discussed in §3.2.

When composites containing conductive fillers are compressed the separation of the filler particles is reduced and the resistance is expected to fall. Such piezoresistance has been observed for many different composites, see refs. 14-16 and the following examples. The resistance of epoxy-graphite composites is reported to fall by a factor of about 100 when subjected to hydrostatic pressure of between 1 and 1.8 GPa.[13] Larger variation has been reported for model composites comprising mixtures of physically separate polymer and conductive powders, when mechanical deformation of either the insulating or conducting particles leads to a pressure-induced percolation transition.[26] For a polymer-soot mixture a 200-fold decrease in resistance is observed, while a polymer-graphite mixture a ca. 10^7 fold decrease occurred. These changes were, however, irreversible due to the nature of the mixtures used. Much smaller changes, a 4-fold decrease for a uniaxial compression of 2 MPa, have been observed in natural rubber-carbon black composites.[27] An exception to this general behaviour is the observation of an increase in resistance by ca. 10^3 times of a polyisoprene-nano-particulate carbon composite under uniaxial compression. [28] This has been attributed to the disruption of the extended structures of the nano-particulate carbon when the composite was deformed. A small initial decrease in resistance up to a compression of ca. 10% followed a larger increase has been reported, and theoretically modelled, for carbon black-silicone rubber composites with carbon black concentrations above the percolation threshold. [29] The changes induced by pressure in QTC samples are in the direction expected but are much larger and show better reversibility than for the examples given above.

The resistance of stretched samples was also observed to fall with deformation, an example is shown in Fig. 2. The circles drawn round the data points encompass the measurement errors. Within experimental error there is an exponential dependence of resistance on elongation indicate by the straight line plotted in Fig. 2. In the light of previous work, discussed below, this is an unexpected result. As noted in §2 the centre of the sample contracted laterally. Although this is proportionately less than the main distortion it must play a role in the observed reduction in resistance with elongation of the sample.

When a composite is subjected to tensile forces the filler particle separation will increase in the direction of elongation and the resistance will be expected to increase. Provided the elastic limit is not exceeded extension of polymer-carbon black composites leads to a reversible increase in resistance. The changes are also modest; less than 8 times for silicone-carbon black,[22] and a similar variation was reported for a latex-fibre composite containing polypyrrole coated cellulose fibres.[23] The polyisoprene-nano-particlate carbon composite mentioned above, where it is thought that the filler morphology is affected by deformation, has a larger reversible increase of 10^4 times. [28] A similar variation is reported for a nickel coated graphite fibre-natural rubber composite but no information was given concerning reversibility.[16] Deformation beyond the elastic limit has been observed to result in a decrease in the resistance of samples due to the alteration in the structure of the composite, but the changes are irreversible. [30, 31] A decrease in resistance has also been reported for a silicone-nickel fibre composite under cyclic loading. [32] However, the effect was only observed during the first five stress cycles after which the resistance increased irreversibly. These changes were attributed to an initial alignment of the nickel fibres followed by mechanical breakdown of the polymer fibre interface. Thus, there appear to be no examples of a large reversible decrease in resistance for composites under tensile stress other than QTC. The changes observed in QTC subjected to elongation are in the opposite sense to that expected. Possible causes of this effect are discussed in §3.2.

The data shown in Fig. 3 was obtained by bending a 1mm thick QTC sample over cylinders of different radii. The resistance is plotted against the inverse of the bend radius since this is a measure of the strain in the surface of the sample. There is negligible deformation of the sample parallel to the axis of bending. When the QTC samples are bent the outer surface is subjected to elongation similar to that shown in Fig. 2 and the measured resistances are also similar. However, at the smallest bending radii there is significant radial compression. Although the data is limited the lines plotted in Fig. 3 suggest different approximately exponential dependencies in the low strain regime and when radial compression occurs. There is no comparative data in the literature on the effect of bending on the resistance of other composites.

The large changes in resistance that occur when QTC samples are deformed provide a sensitive measure of the creep of the polymer matrix when a sample is subjected to a constant tensile stress. This is avoided in the measurements described above by using fixed deformations rather than fixed forces and allowing samples to relax to a constant resistance before measurements are made. The changes in resistance with deformation are reversible with only small hysteretic effects. The data for compression, elongation and bending indicates that the resistance of QTC samples varies exponentially with strain and that the physical mechanism underlying this unusual behaviour is similar in these situations.

3.2 Particle morphology and conduction mechanism

The most distinct difference between QTC and the other composites described above is the morphology of the filler articles in the composite. The Inco nickel particles have an extremely spiky morphology with numerous sharply pointed protrusions and ridges. This morphology is designed to produce a free flowing powder suitable for powder metallurgy. The careful mixing of filler and precursor monomer is designed to avoid damaging the nickel filler particles. The nickel particles will have a thin native oxide layer. However, this grows extremely slowly in air at room temperature and the properties of the composite are unaffected by storage of the powder for several years prior to use, indicating that any oxide layer present affects neither the particle morphology nor the conduction process.

SEM and TEM examination of QTC shows that the original sharp projections on the surface of the filler particles are retained in the as-made composite. SEM images of freeze-fractured samples show that the filler particles are intimately coated with the silicone polymer matrix, Fig. 4(a). The coating of polymer obscures the sharp surface features of the particles. When a high accelerating voltage is employed to give greater penetration of the electrons into the polymer, the underlying structure of the nickel particles is discernable in secondary electrons images, Fig 4(b). The SEM images show a high density of nickel particles, commensurate with the high filler loading. The particles are randomly distributed with an approximately constant density over areas of ca. 10^{-8} m^2 but with local fluctuations in density on a smaller scale; see Figs

4(a) and 5. More direct evidence of the particle morphology is provided by TEM images, Fig. 5. The protrusions visible in profiles of the particles shown in Fig. 5(a) show that the particle morphology has not been changed significantly during the fabrication of the composite. In a few samples where the projections of the nickel extend beyond the microtomed surface, pyramidal and filamentary projections with tip radii of 10 nm and less are observed, Fig. 5(b) and (c). These sharp features are similar to the tips utilised in scanning tunnelling microscopes (STMs).[33] Inter-particle separation varies over a wide range but many particles are seen to have separations well below 100 nm.

On the basis of these observations the following model can be proposed for conduction in QTC. The intimate coating of the particles prevents them from coming into direct physical contact, hence the high resistance of the as-made composite despite the filler loading being above the expected percolation threshold. The high filler loading means that there are many pathways that, in the absence of the polymer coating, would be a percolation path. Charge injected into the composite will reside on the filler particles and give rise to high local fields at the tips of the extremely sharp surface features. These tips are likely to have field enhancement factors as high as 1000.[34] This will favour field enhanced emission, Fowler-Nordheim tunnelling. Direct evidence for the occurrence of high fields at the spikes on the filler particles is provided by the observation of localised discharge to air from the side of compressed cylindrical samples, diameter 10 mm, connected to a 240 V AC source. This requires that fields greater than 3×10^6 Vm^{-1} occur at the tips of the sharp features on the filler particles in QTC. When the composite is deformed the average particle separation along the putative percolation paths will be reduced, i.e. most particles are in close enough proximity that field induced tunnelling can occur from the sharp surface features.

The exponential dependence on deformation shown in Figs. 1, 2 and 3 support a model of conduction dominated by a tunnelling process. In samples compressed to low resistance the already densely packed nickel particles are brought into close proximity. This, together with the spiky particle morphology, means that inter-particle interaction will increase the stiffness of the composite. Such stiffening is observed

experimentally and explains the deviation from exponential behaviour at high compression seen in Fig. 1. The unexpected observation of a decrease in sample resistance in extension can also be attributed to the high filler concentration. The effect of uniaxial deformation can be modelled in terms of contributions due to changes in filler particle separation parallel and perpendicular to the direction of the applied force.[29] Percolation paths are randomly distributed in a composite so that there are more contacts between particles in the perpendicular than in the parallel direction. Because of this the model predicts that, in the percolation regime, although the perpendicular deformation is smaller than the parallel deformation it is the dominant factor determining the response of the composite to deformation as observed experimentally. Thus, when QTC is stretched the reduction in particle separation in the putative percolation paths perpendicular to the stretching direction must dominate over increasing separation in the parallel direction. The occurrence of field induced tunnelling means that carriers can traverse larger gaps than in a conventional composite. This further suppresses the effect of the increasing particle separation in the parallel direction. The large perpendicular deformations and consequent inhomogeneity of the composite may also contribute to the continuous reduction in sample resistance seen in Fig. 2. Similar effects will be important in the reduction of resistance in bent samples.

The corollary to this conclusion is that these properties are not seen in conventional composites since the filler particles either lack very sharp surface protrusions, or are not intimately coated with polymer, or both. The vigorous mixing normally used to make composites would destroy the fine surface morphology of the filler particles and grind them down to a spherical shape. To test this hypothesis samples were made using the same filler and matrix but either subjecting the mixture to different degrees of vigorous mixing, or milling the filler prior to formation of the composite. Pressure-resistance curves for a series of these samples are shown in Figs. 6(a) and (b) respectively. This shows that the composites that contain damaged filler particles become progressively less sensitive to the applied force. Electron microscope examination revealed that this loss of sensitivity was associated with the removal of the sharp spikes and edges from the filler particles, Figure 7. The sensitivity of QTC™ is also reduced by either oxidizing the Ni filler, by heating the powders in air

between ca. 550ºC and 750ºC for several hours, or etching it with 30% HCl. Both treatments are likely to attack the spikes on the filler particles. SEM images of the nickel powder before and after etching show a significant reduction in the number of sharp features. These results provide further support for the model proposed above.

3.3 Current-voltage characteristics

QTC™ displays extremely non-linear current-voltage characteristics, which are explicable in terms of the model proposed above. These characteristics are not fixed but depend on the initial deformation of the sample, i.e. the initial resistance, the maximum voltage applied to the sample and the sample history. The initial resistance was determined from the initial slope of the current-voltage curve. Fig. 8 shows examples of current- voltage characteristics for samples under low compression, with initial resistances > 1 Mohm, and low data collection rate. The characteristic shown in Fig. 8(a) is typical of samples with initial resistances greater than a few hundred ohm. Initially the current increases super-linearly with applied voltage. The rate of increase then falls until a maximum current is reached beyond which the current then falls with increasing voltage. This negative resistance regime is characterised by apparently random fluctuations in the current. On decreasing the applied voltage from its maximum value there is marked hysteresis. The current increases slowly as the voltage is reduced, and in some instances remains approximately constant over a wide voltage range, before increasing rapidly over a narrow voltage range. Finally the current falls non-linearly to zero as the voltage is reduced to zero. The final resistance is lower than the initial resistance. In a few instances the increase in current during the reduction in applied voltage occurs extremely rapidly, as shown in Fig. 8 (b).

Such highly non-linear behaviour has not previously been observed in conductive composites. Generally carbon black filled composites show ohmic behaviour unless there is sufficient Joule heating for the positive temperature coefficient of resistance to have an effect, when a small negative resistance regime can be observed.[35] There are a few reports of non-linearity in the absence of heating. van Beek and van Pul [18] reported an exponential dependence of current on voltage for high resistance samples, typically greater than 10^5 ohm, and high applied fields, up to 6×10^6 Vm^{-1}. This data

was interpreted in terms of internal field emission. Celzard et al [24] studied graphite flake-epoxy composites with compositions just above the percolation threshold and found a reversible current-voltage characteristic given by the sum of linear and quadratic voltage terms. This was interpreted in terms of a non-linear random resistor network formed by the contacts between the graphite flakes. These effects are all significantly weaker than the non-linearity observed in QTC.

The trend in the form of the current-voltage characteristic as the initial resistance is reduced is illustrated in Fig. 9. The initial resistances are approximately 100 kohm, Fig. 9(a), 900 ohm, Fig. 9(b) and 10 ohm, Fig 9(c). On the initial voltage sweeps the behaviour is as described above except for the highly compressed, low resistance, sample where the response is initially ohmic but followed by regions of sub- and super-linear voltage dependence. At highest voltages the current decreases to very small values in all cases. A high sample rate was used for data collection and the fluctuations in current are seen to start before the maximum current is reached, and continue until current flow is suppressed. The maximum in the current that occurs as the voltage is decreased is reduced as sample compression increases. At the low compressions, and high initial resistances, the final resistance is lower than the initial resistance but at high compression and low initial resistance the situation is reversed. Data for a series of samples indicates that the ratio of initial and final resistances depends on the initial resistance to the power *n*, where *n* is of the order 0.8, Fig. 10. Thus, the effect is most marked for the more resistive samples. The fact that not all samples were driven until current flow was suppressed, i.e. the amount of trapped charge was not maximised, see Fig. 8 and 9, is a partial explanation for the scatter in the data in Fig. 10.

The observations noted in § 3.2 supporting the model of Fowler-Nordheim tunnelling indicate that charge is stored on the Ni particles. We attribute the negative resistance regime to charge storage on the metal particles. The random particle shape and distribution means that along the conduction paths there will be a distribution of potential barriers affecting charge transport. Charge can build up on a particle where there is a high barrier for charge flow in the field direction, i.e. a large separation to the next particle in the conduction path that acts as a dead-end. The trapped charge

will produce an enhanced local field that will create potential barriers in adjacent conduction paths. Trapping of charge on the adjacent paths provides a feedback mechanism that pinches off conduction paths, causing the current through the sample to fall. The charge distribution established while the applied voltage is increased persists as the voltage is reduced. Eventually the applied field is no longer large enough to maintain the distribution of trapped charge and it is redistributed, but not eliminated. The residual trapped charge leaves the sample with a resistance different from that in the initial uncharged state. The stored charge gives rise to internal forces between the Ni particles and there will be a mechanical response due to the deformation of the elastomeric polymer matrix.[36] This effect will contribute to the changes in the conductive pathways in the QTC that occur during voltage sweeps. It will also alter the microscopic geometry of samples that retain charge after a voltage sweep. Thus, in a charged sample the geometry of the sample and the conduction paths are different from the initial configuration. This accounts for the hysteresis that occurs when the applied voltage is reversed and the difference in initial and final resistance of cycled samples.

Evidence for local charge redistribution within the QTC during voltage sweeps has been provided by direct observation of current transients with a fast oscilloscope, Tektronix TDS350. These data reveal charge oscillations with frequencies between 1 and 30 MHz, Fig. 11. These occur principally at higher voltages in the region where the current flow through the composite is reduced, and to a lesser extent in the first negative resistance regime. It is apparent from Fig. 8, 9 and 11 that charge redistribution occurs in QTC on all levels from the microscopic to the macroscopic.

The presence of this trapped charge is also revealed by the behaviour of subsequent current-voltage sweeps, which depend on the time that has elapsed since the initial measurement. On an immediate repeat the current follows the characteristic observed on the first down sweep of voltage and can be cycled into the negative resistance regime. If a few days are allowed to elapse, during which the stored charge can leak away, the initially observed behaviour is recovered. The initial behaviour is also recovered by compressing the sample to a low resistance, which allows the stored charge to leak away rapidly, returning the sample to its initial high resistance state.

The low resistance state can also be triggered in uncompressed samples by the application of a high voltage impulse, which creates a conductive region where charge is deposited by the impulse. The mechanical response of QTC to trapped charge can account for this. The deposited charge will be distributed along the least resistive pathways before being trapped; the trapped charge will then deform the composite, affecting the inter-particle separation in the vicinity of the trapped charge. These results provide a clear indication that the effects observed are due to charge storage on the Ni particles in the QTC. It is also likely that the rapid changes in sample resistance observed in both the regions of negative resistance on the up and down voltage sweeps, Fig. 8 and 9, are the result of a rapid redistribution of charge coupled to the mechanical response of the matrix.

Finally we note that the initial section of the current-voltage characteristic of QTC can be compared to that observed in polycrystalline ceramic varistors.[37, 38] In these an initial high resistance regime occurs due to the presence of potential barriers at the grain boundaries. As the fields across these boundaries increase, field induced emission occurs and the conductivity of the varistor increases rapidly as a function of applied voltage. At the highest fields the resistance approaches a value determined by the resistance of the ceramic particles. Fig. 12 shows a log-log plot of voltage versus current, as conventionally used for varistors, for QTC samples with different initial resistances. At low compression, i.e. high sample resistance, the characteristic of QTC is similar to that of a varistor up to the point that the current in the QTC falls in the negative resistance regime. This similarity lends further support to the model of field induced tunnelling in QTC. Fig. 12 shows the similarity becomes less pronounced and is eventually lost as sample compression is increased. This is to be expected since the separations of the metallic grains are reduced, charge transport is facilitated so that trapping of charge is inhibited and ohmic behaviour is observed. The behaviour of QTC on repeated voltage cycles is complex and will be discussed in greater detail in a separate paper.

3.4 Sensitivity to organic vapours

The use of carbon black composites as elements for incorporation in vapour sensor arrays has been reported.[39, 40] Absorption of vapours leads to swelling of the host polymer and causes changes in the sensor resistance. An array of such sensors can be used, together with suitable data analysis, as an "electronic nose". The sensitivity of the Peratech composites to deformation, described in §3.1, indicates that they should be suitable materials for this type of vapour sensor. A large response has been observed to a range of volatile materials, examples are shown in Fig. 13. Sensors were made from a granular form of QTC™ with a nickel loading of 10:1 by weight. Vapour was passed through a porous bed of granules compressed between two nickel gauze meshes, which acted as electrical contacts. The increase in resistance is due to the homogeneous expansion that results from the swelling of the polymer matrix by the organic vapour. Further results on vapour sensing with QTC will be presented elsewhere.

4. Conclusions.

The retention of sharp features on the surfaces of the nickel particles in polymer matrix composite, QTC™, has been verified by transmission electron microscopy. Scanning electron microscope images of freeze-fracture surfaces reveal that the matrix polymer intimately coats the nickel particles. Because the adhering polymer separates the metal particles the composite has a very high resistance even when the quantity of nickel powder incorporated in the composite is above the percolation threshold. The resistance of the composite is found to be extremely sensitive to any mechanical deformation. Thus, unlike other conductive composites the resistance falls when the material is either stretched, or bent, or twisted. Modest applied forces produce resistance changes of many orders of magnitude.

The experimentally observed exponential dependence of sample resistance on deformation indicates that the principal conduction mechanism is by carriers tunnelling between the filler particles. The reduction in response to mechanical deformation when the sharp surface features are damaged provides circumstantial evidence that field enhanced emission, i.e. Fowler-Nordheim tunnelling, occurs. The observation of discharges to air from QTC™ samples shows directly that very large

fields are generated on the surfaces of the undamaged filler particles. The composites display extremely non-linear, hysteretic, current-voltage characteristics, which are dependent on the initial conditions and sample history. The hysteresis and history dependence are attributed to charge trapped in the composite, which leaks away slowly unless the sample resistance is reduced to a low value by compression.

The results presented here emphasise the unique properties of QTC™, which are unlike those of composites previously investigated in either industry or academia. The extreme sensitivity of QTC™ to deformation renders it suitable for a number of applications including switches, tactile sensors[41] and sensors for volatile organic compounds.

5. Acknowledgements.

The EPSRC is thanked for a grant in aid of part of this work and for a postgraduate studentship for P.J.W. Hands. R. Gordon and R.C.J. de Vincent-Humphreys are thanked for measurements taken during their final year undergraduate projects.

References

1. R.H. Norman, Conductive Rubber, Maclaren (1957).
2. S.K. Bhattacharya and A.C.D. Chaklader, Polym. Plast. Technol. Eng., **19**, 21 (1982).
3. V.E. Gul', Structure and Properties of Conducting Polymer Composites, VSP, Utrecht (1996).
4. R. Strümpler and J. Glatz-Reichenbach, J. Electroceram., **3:4**, 329 (1999).
5. F. Carmona, Physics A, **157**, 461 (1989).
6. D.S. McLachlan, J. Electroceram., **5:2**, 93 (2000).
7. L. Flandin, T. Prasse, R. Schueler, K. Schulte, W. Bauhofer and J-Y. Cavaille, Phys. Rev. B, **59**, 14349 (1999).
8. I. Balberg, Carbon, **40**, 139 (2002).
9. M.T. Connor, S. Roy, T.A. Ezquerra and F.J. Baltá Calleja, Phys. Rev. B, **57**, 2286 (1998).
10. B. Sixou and J.P. Travers, J. Phys. C.: Cond. Mat. Phys., **10**, 593 (1998).
11. P. Sheng, Phys. Rev. B, **21**, 2180 (1980).
12. J.C. Dawson and C.J. Adkins, J. Phys. C.: Cond. Mat. Phys., **8**, 8321 (1996).
13. A. Celzard, E. McRae, J.F. Marêché, G. Furdin and B. Sundqvist, J. Appl. Phys., **83**, 1410 (1998).
14. C. Grimaldi, T. Maeder, P. Ryser and S. Strässler, Phys. Rev. B, **67**, 014205 (2003).
15. J.E. Martin, R.A. Anderson, J. Odinek, D. Adolf and J. Williamson, Phys. Rev. B, **67**, 094207 (2003).
16. M. Taya, W.J. Kim and K. Ono, Mech. of Mater., **28**, 53 (1998).
17. R. Strümpler, G. Maidorn and J. Rhyner, J. Appl. Phys., **81**, 6786 (1997).
18. L.K.H. van Beek and B.I.C.F. van Pul, J. Appl. Polym. Sci., **6**, 651 (1962) and Carbon, **2**, 121 (1964).
19. S.Miyauchi and E.Togashi, J.Appl.Polym.Sci., **30**, 2743 (1985).
20. S. Radharkrishnan, Polym. Commun., **26**, 153 (1985).
21. Peratech Ltd., UK Patent PCT/GB98/00206 (WO 98/33193).
22. J. Kost, M. Narkis and A. Foux, Polym. Eng. and Sci., **23**, 567 (1983).
23. L. Flandin, Y. Bréchet and J-Y. Cavaillé, Comp. Sci. & Tech., **61**, 895 (2001).

24. A. Celzard, G. Furdin, J.F. Marêché and E. McRae, J. Mater. Sci., **32**, 1849 (1997).
25. R.G.Longoria, http://www.me.utexas.edu/~lotario/me244L/leks/sensors/rsensors.pdf
26. T. Chelidze and Y. Gueguen, J.Phys.D: Appl. Phys., **31**, 2877 (1998).
27. A.E. Job, F.A. Oliveira, N. Alves, J.A. Giacometti and L.H.C. Mattoso, Synth. Metals, **135-136**, 99 (2003).
28. M. Knite, V. Teteris, A. Kiploka and J. Kaupuzs, Sensors & Actuators A, **110**, 142 (2004).
29. N. Ryvkina, I. Tchmutin, J. Vilčáková, M. Pelíšková and P. Sáha, Synth. Metals, **148**, 141 (2005).
30. L. Flandin, A. Chang, S. Nazarenko, A. Hiltner and E. Baer, J. Appl. Polym. Sci., **76**, 894 (2000).
31. L. Flandin, A. Hiltner and E. Baer, Polymer, **42**, 827 (2001).
32. X. Shui and D.D.L. Chung, Smart Mater. Struct., **6**, 102 (1997).
33. C. Bai, Scanning Tunneling Microscopy and its Applications, Springer Ser.Surf.Sci., **32**, Springer Verlag, Heidelberg (2000).
34. C.J. Edgecombe and U. Valdre, J. of Microscopy, **203**, Pt. 2, 188 (2001).
35. F. El-Tantawy, K. Kamada and H.Ohnabe, Mater. Lett., **56**, 112 (2002).
36. R.Pelrine, R. Kornbluth. J. Joseph, R. Heydt, Q. Pei and S. Chiba, Mater. Sci. & Eng. C, **11**, 89 (2000).
37. L.M. Levinson and H.R. Philipp, J. Appl. Phys., **46**, 1332 (1975).
38. B. Birner, J. Nonlin. Maths. Phys., **5**, 331 (1998).
39. M.C.Lonergan, E.J.Severin, B.J.Doleman, S.A.Beaber, R.H.Grubbs and N.S.Lewis, Chem.Mater, **8**, 2298 (1996).
40. B.J.Doleman, M.C.Lonergan, E.J.Severin, T.P.Vaid and N.S.Lewis, Anal.Chem., **70**, 4177 (1998).
41. T.B.Martin, NASA Tech. Briefs, **28**, Oct 2004 p. 29.

Figure Captions

Figure 1 Variation in resistance as a function of compression for a soft silicone-Ni type 123 QTC™ composite (5:1 Ni by weight in a 40% Silastic T4, 60% GE RTV 6166 matrix). Measurement error is indicated by the size of the circles enclosing the data points. Experimental set up with deformed sample is shown in insert, see text for details.

Figure 2 Variation in resistance as a function of elongation for a silicone-Ni type 287 QTC™ composite (4:1 Ni by weight in a Alphasil 2000 matrix). Measurement error is indicated by the size of the circles enclosing the data points. Experimental set up with deformed sample is shown in insert, see text for details.

Figure 3 Variation in resistance as a function of bending radius for a silicone-Ni type 123 QTC™ composite (5:1 Ni by weight in a Silcoset 153 matrix). The error in bending radius is shown and the circles enclosing the data points indicated the error in the resistance values. Experimental set up with deformed sample is shown in insert, see text for details.

Figure 4. Scanning electron microscope images of freeze-fracture sections of QTC™ composites. (a) A normal image of a silicone-Ni type 123 QTC™ composite (6:1 Ni by weight in Alphasil 2000) and (b) a secondary electron image of a silicone-Ni type 287 QTC™ composite (4:1 Ni by weight in Alphasil 2000). The scale bars indicate the magnification.

Figure 5. Transmission electron microscope image of a silicone-Ni type 287 QTC™ composite (4:1 Ni by weight in Alphasil 2000): (a) a microtomed section, (b) and (c) a free surface with a projecting spike on the surface of a Ni particle. The scale bars indicate the magnification.

Figure 6. Variation in resistance as a function of compression for (a) silicone-Ni type 123 QTC™ composites (4:1 Ni by weight in Alphasil 2000) prepared with either different degrees of energy input during mixing from low, at the left, to high, at the right, and (b) a silicone-Ni type 287 QTC™ composite (5:1 Ni by weight in Silastic T4) with the Ni milled for 40 sec, □, and 60 sec, O.

Figure 7. Scanning electron microscope image of a freeze fracture surface of a silicone-Ni type 123 QTC™ composite prepared with high energy input during mixing (right hand line in Fig 6(a)).

Figure 8. Current-voltage characteristics for a silicone-Ni type 123 QTC™ sample (4:1 Ni by weight in a Alphasil 2000 matrix) compressed to give initial resistances >1 Mohm.

Figure 9. Current-voltage characteristics for silicone-Ni type 123 QTC™ samples (4:1 Ni by weight in a Dow Corning T4 matrix) compressed to give initial resistances, (a) ~100 kohm, (b) ~900 ohm, and (c) ~10 ohm.

Figure 10. Ratio of the final to the initial resistance of compressed silicone-Ni type 123 QTC™ samples (various matrices as given in captions to Figs 8 and 9) as a function of the initial resistance. The fitted line is given by $R_i/R_f \approx 0.08 \times R_i^{0.82}$.

Figure 11. Current oscillations observed in the negative resistance regime of a silicone-Ni type 123 QTC™ sample (4:1 Ni by weight in a Dow Corning T4 matrix).

Figure 12. Log-log plot of voltage versus current for silicone-Ni type 123 QTC™ samples (4:1 Ni by weight in a Dow Corning T4 matrix) compressed to initial resistances of ~100 Mohm, □, 1.4 Mohm, O, 850 ohm, △, and 94 ohm, ◇.

Figure 13. Response of (a) silicone-Ni type 123 QTC™ (10:1 Ni by weight in a Dow Corning T4 matrix) exposed to saturated hexane vapour and (b) polyurethane-Ni type 123 QTC™ (10:1 Ni by weight in a Techsil F42 matrix) exposed to saturated tetrahydrofuran vapour.

Figures

Figure 1.

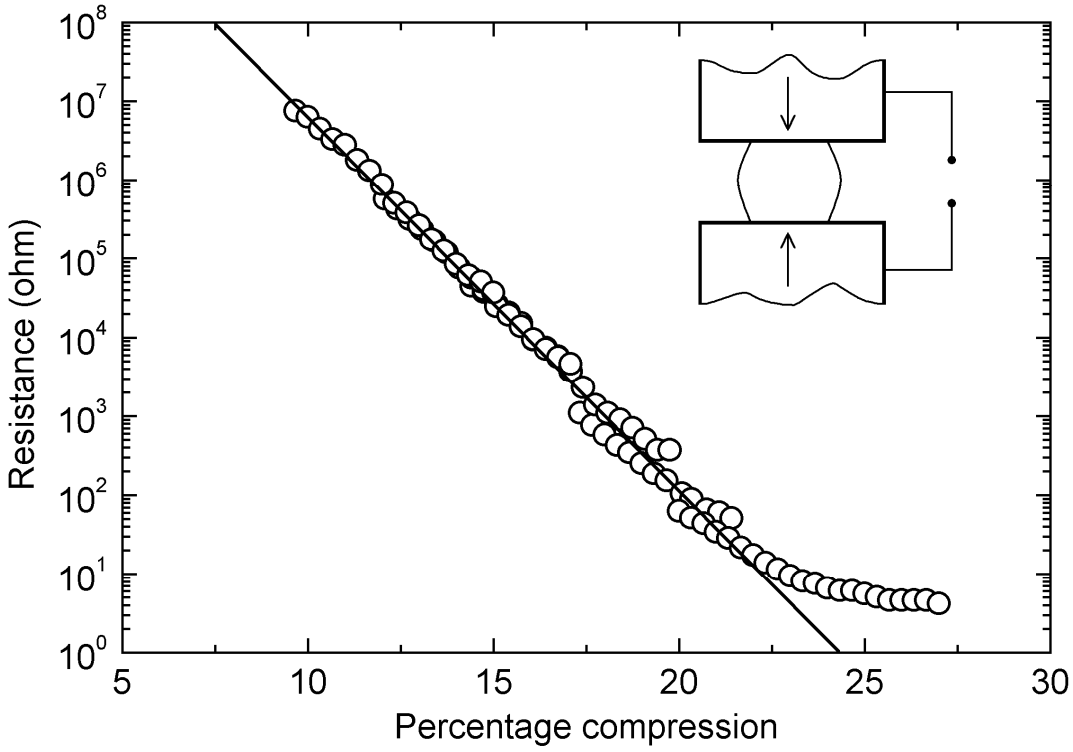

Figure 2.

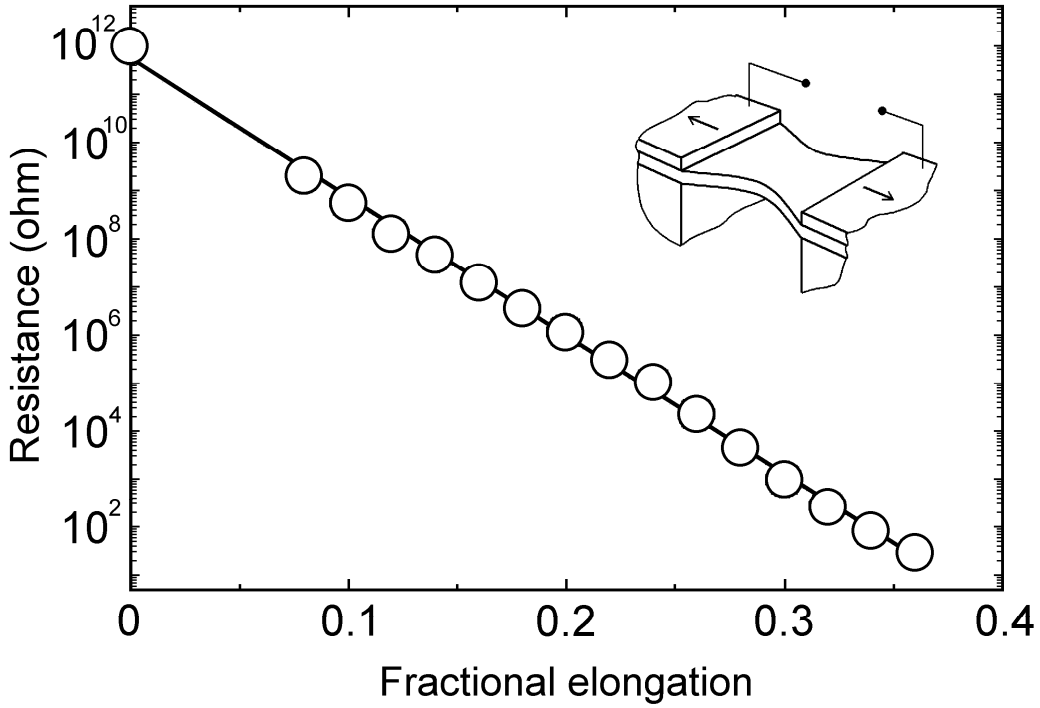
Resistance (ohm)
10^12
10^10
10^8
10^6
10^4
10^2
0
0.1
0.2
0.3
0.4
Fractional elongation

Figure 3.

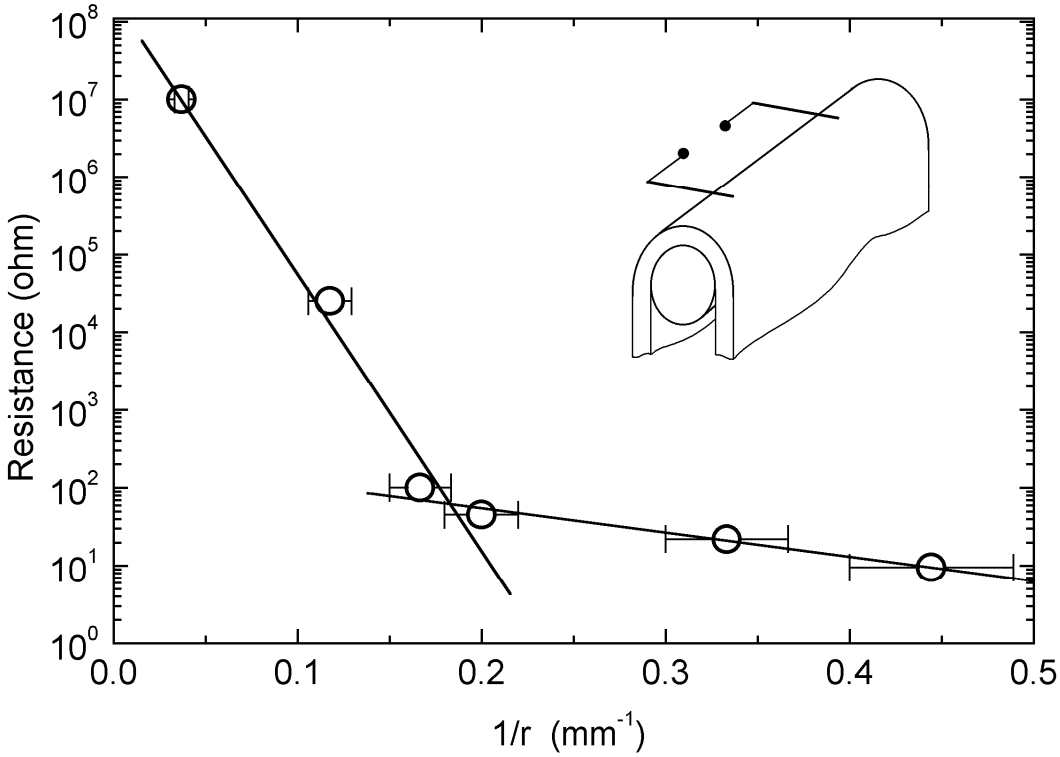
Resistance (ohm)
10^8
10^7
10^6
10^5
10^4
10^3
10^2
10^1
10^0
0.0
0.1
0.2
0.3
0.4
0.5
1/r (mm^{-1})

Figure 4.

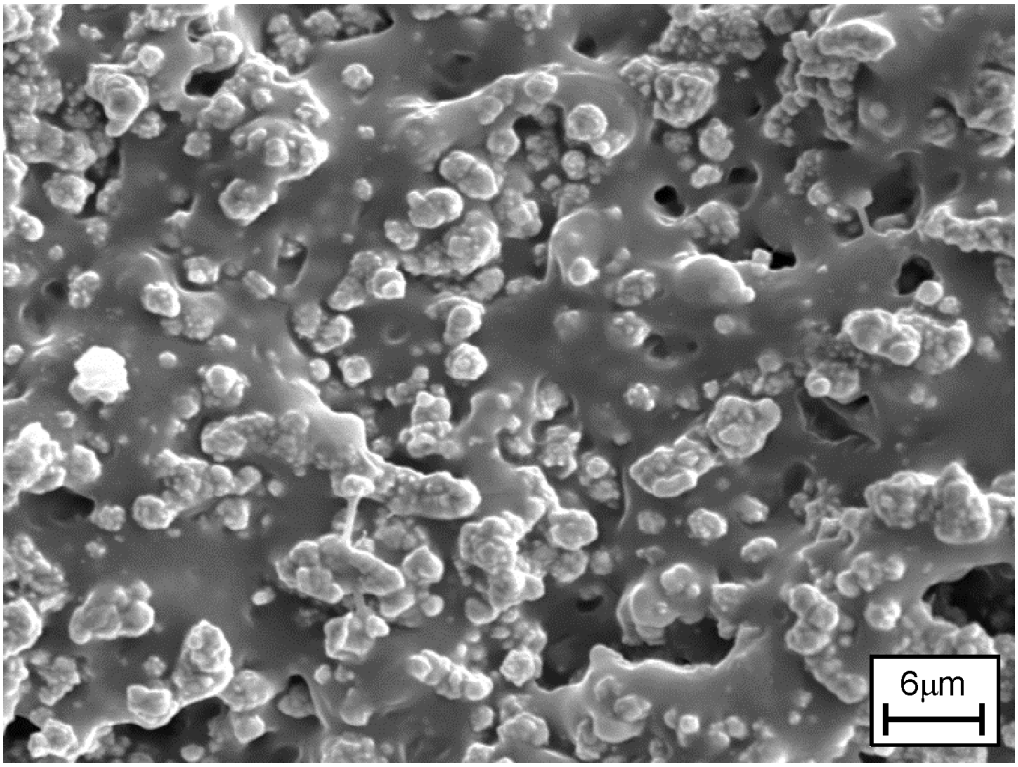

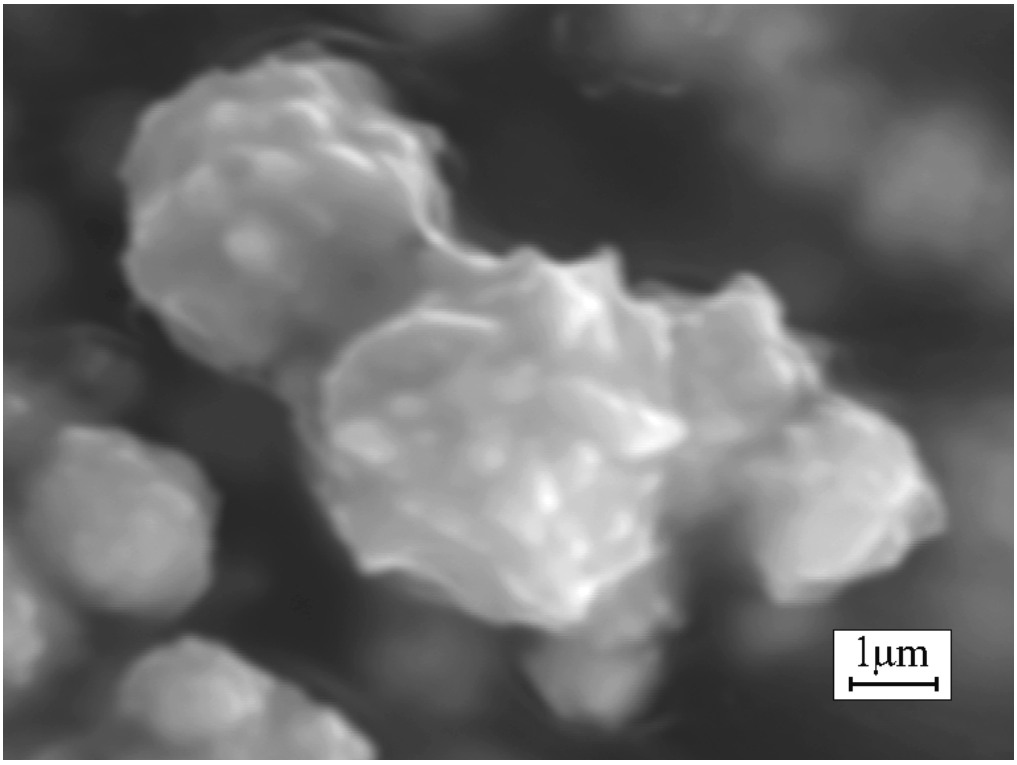

Figure 5.

(a)

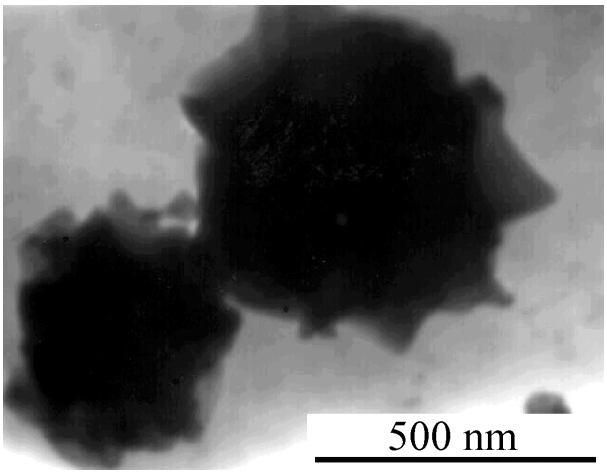

(b)

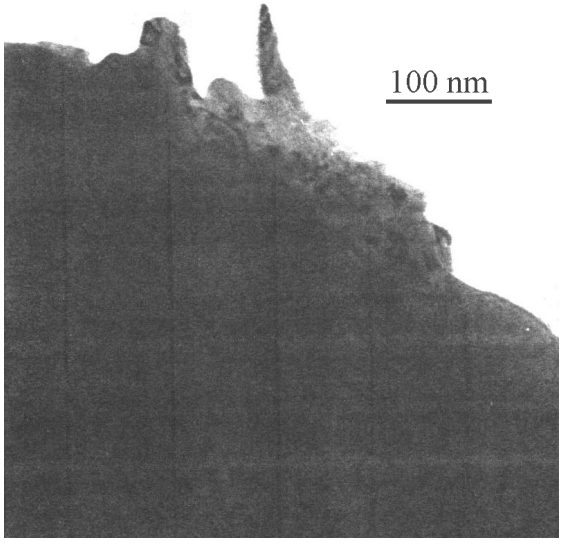

(c)

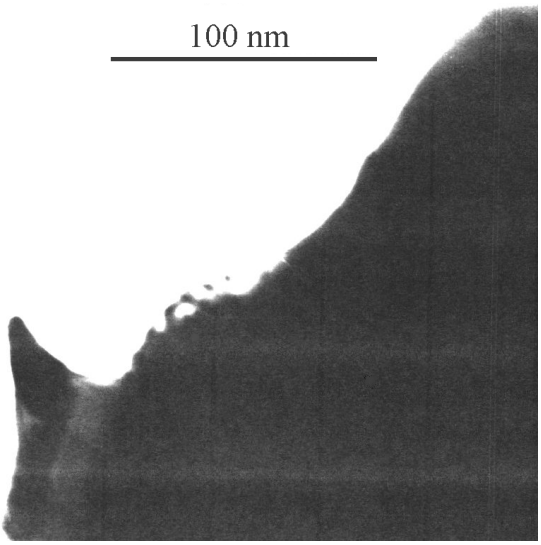

Figure 6.

(a)

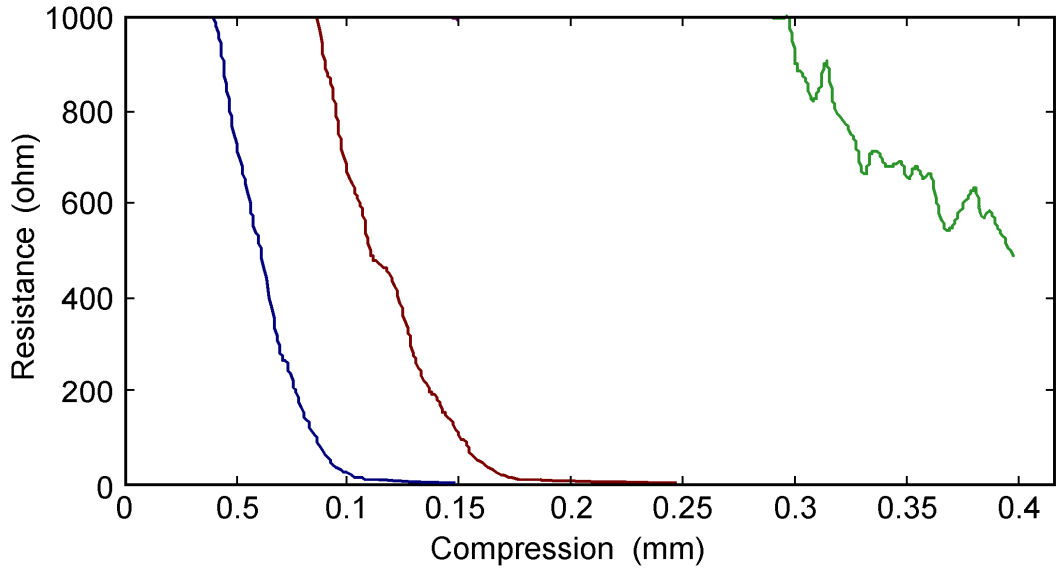
1000
800
600
400
200
0
Resistance (ohm)
0
0.5
0.1
0.15
0.2
0.25
0.3
0.35
0.4
Compression (mm)

(b)

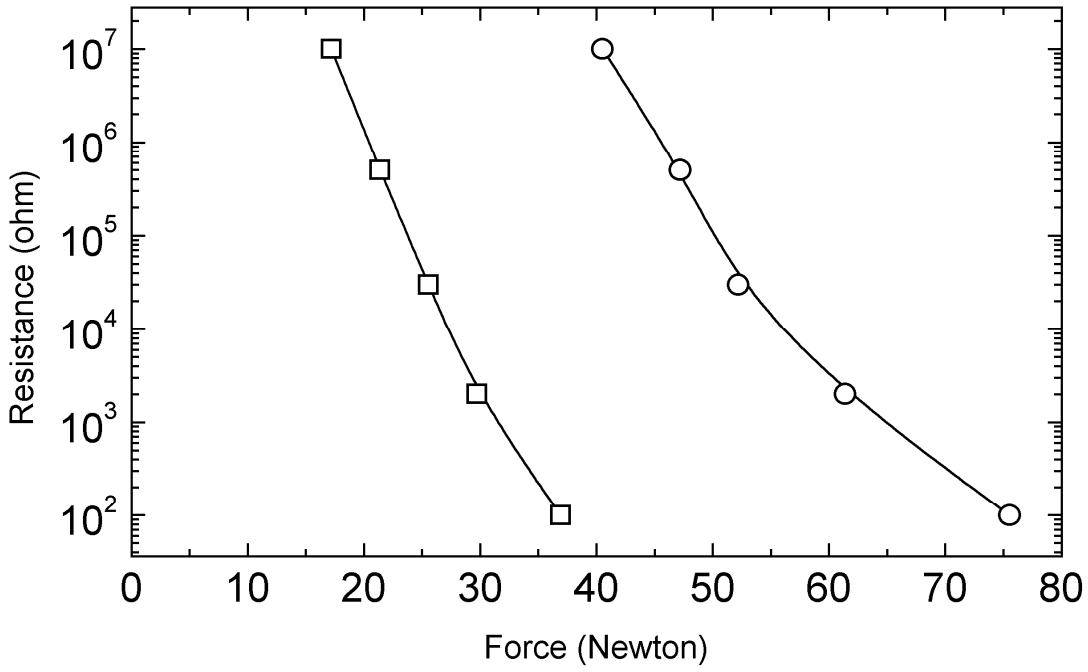
10^7
10^6
10^5
10^4
10^3
10^2
Resistance (ohm)
0
10
20
30
40
50
60
70
80
Force (Newton)

Figure 7.

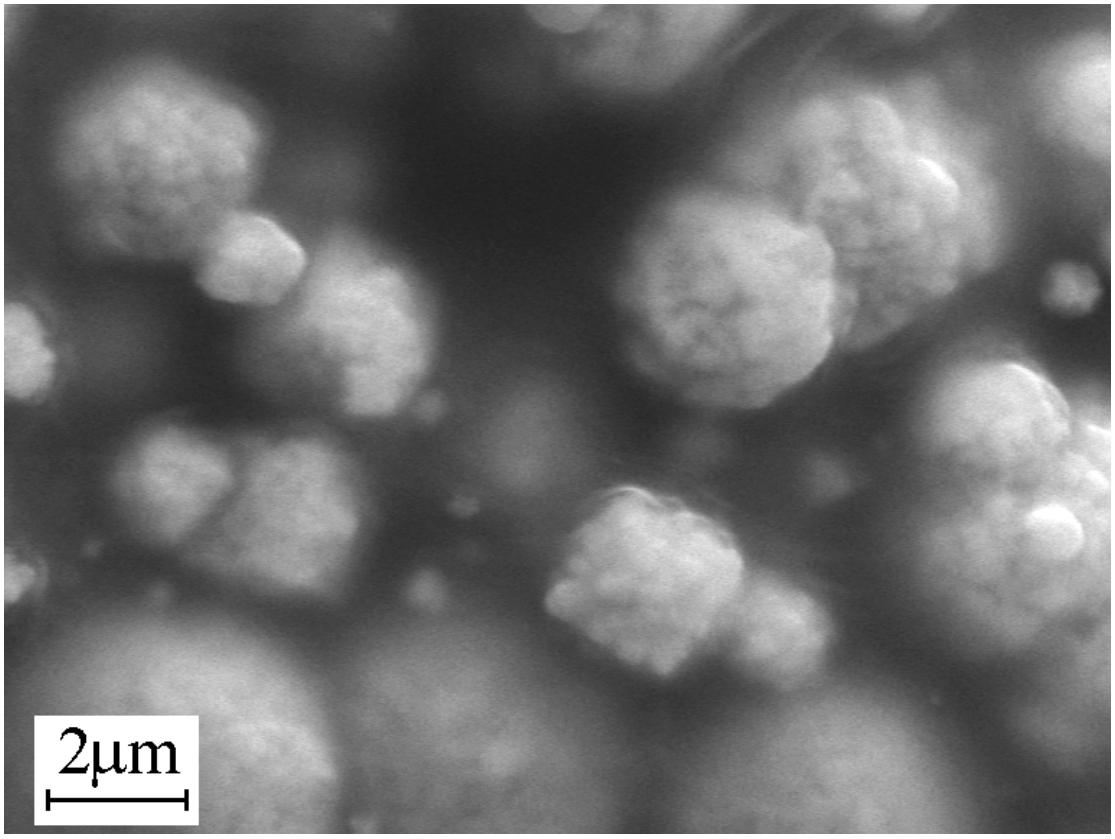

Figure 8.

(a)

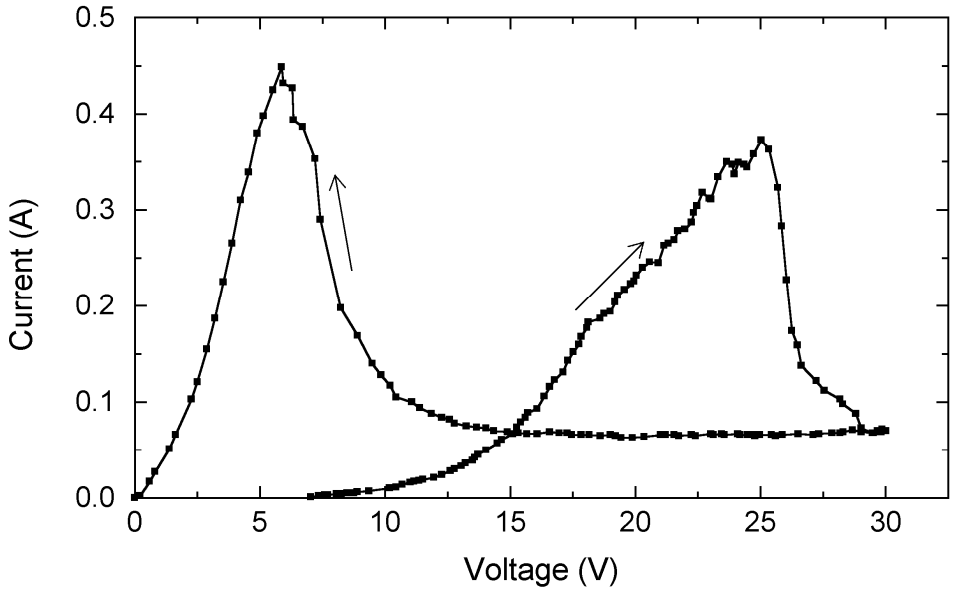
0.5
0.4
0.3
0.2
0.1
0.0
Current (A)
0
5
10
15
20
25
30
Voltage (V)

(b)

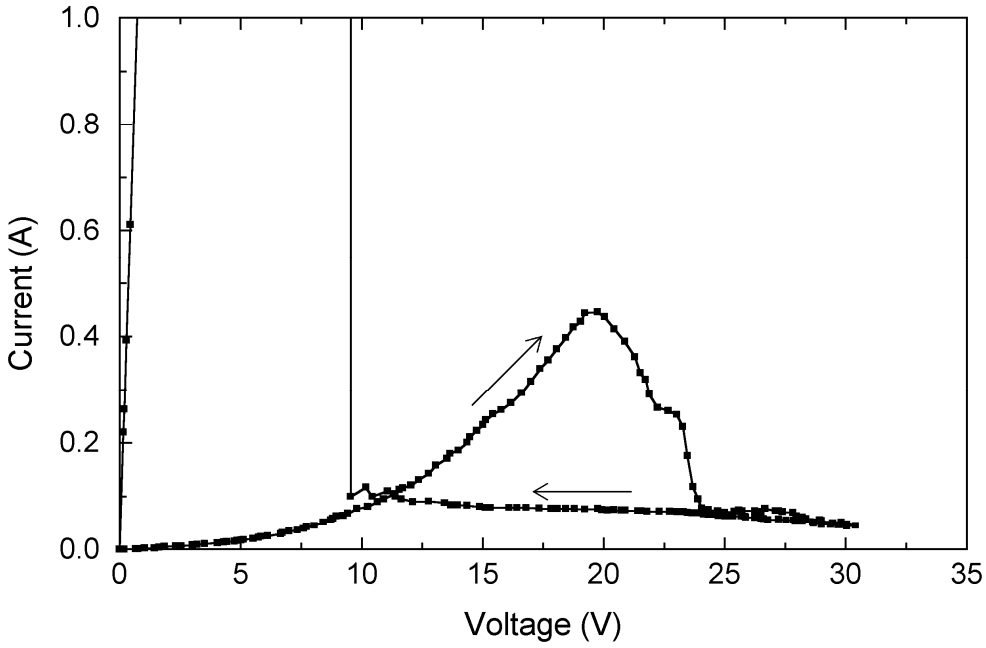
1.0
0.8
0.6
0.4
0.2
0.0
Current (A)
0
5
10
15
20
25
30
35
Voltage (V)

Figure 9.

(a)

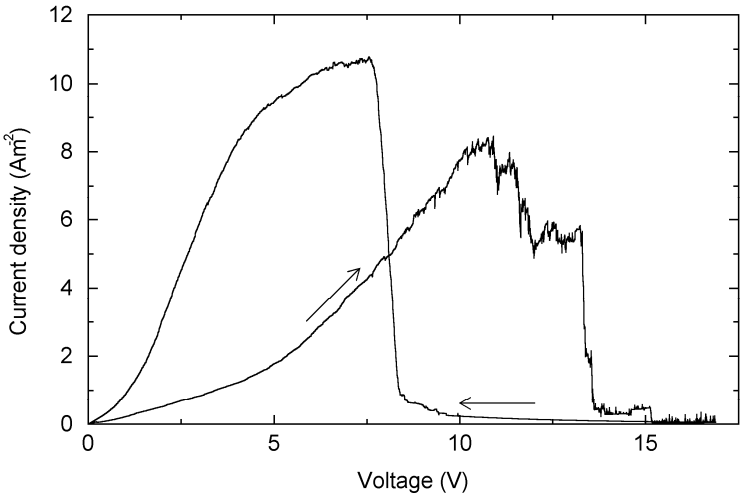
Current density (Am^{-2})
Voltage (V)
0
2
4
6
8
10
12
0
5
10
15

(b)

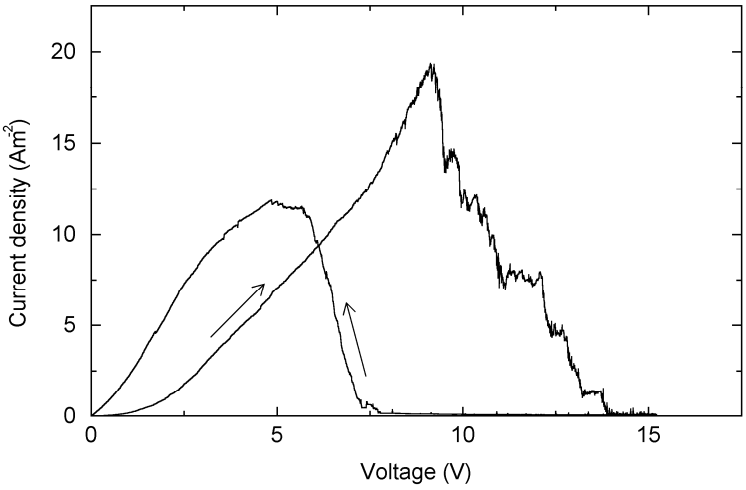
Current density (Am^{-2})
Voltage (V)
0
5
10
15
20
0
5
10
15

(c)

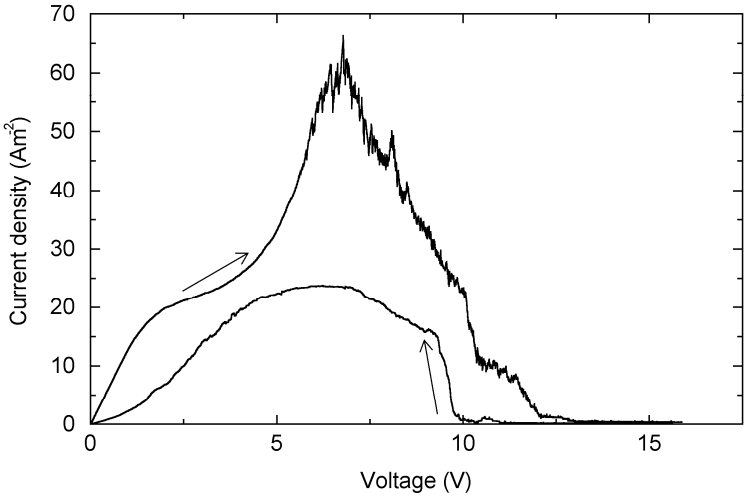
Current density (Am^{-2})
Voltage (V)
0
10
20
30
40
50
60
70
0
5
10
15

Figure 10.

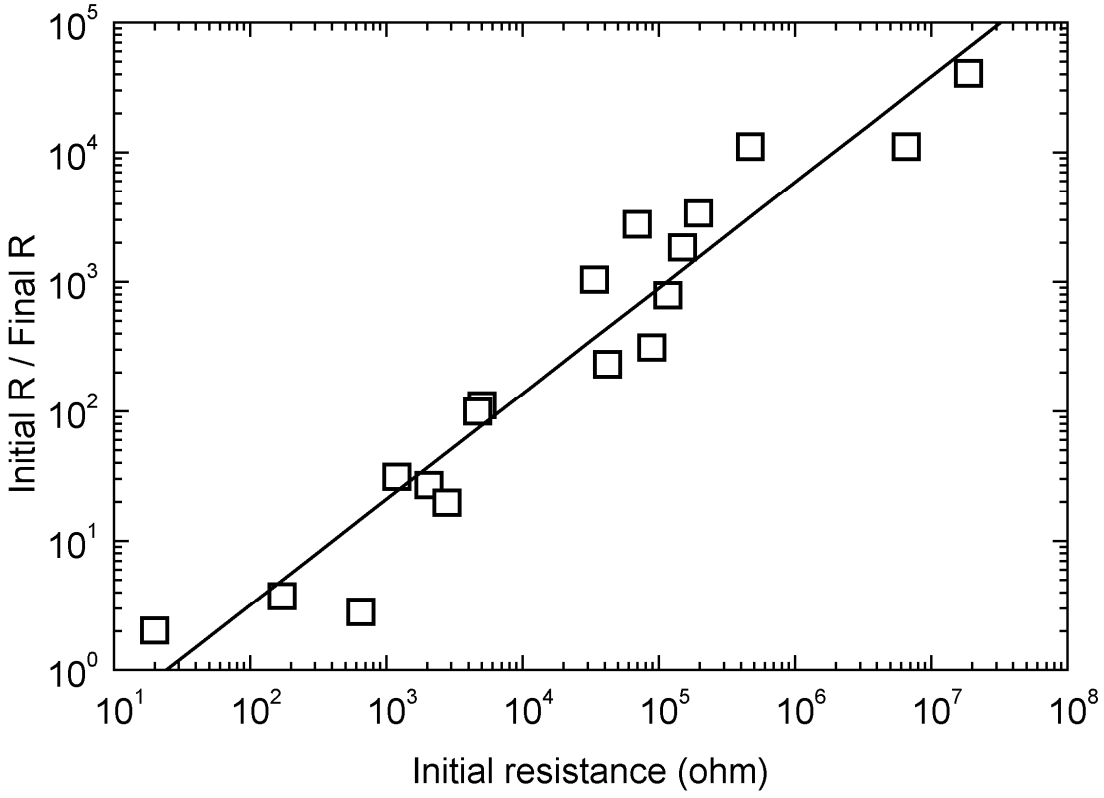
Initial R / Final R
Initial resistance (ohm)
10^0
10^1
10^2
10^3
10^4
10^5
10^6
10^7
10^8

Figure 11.

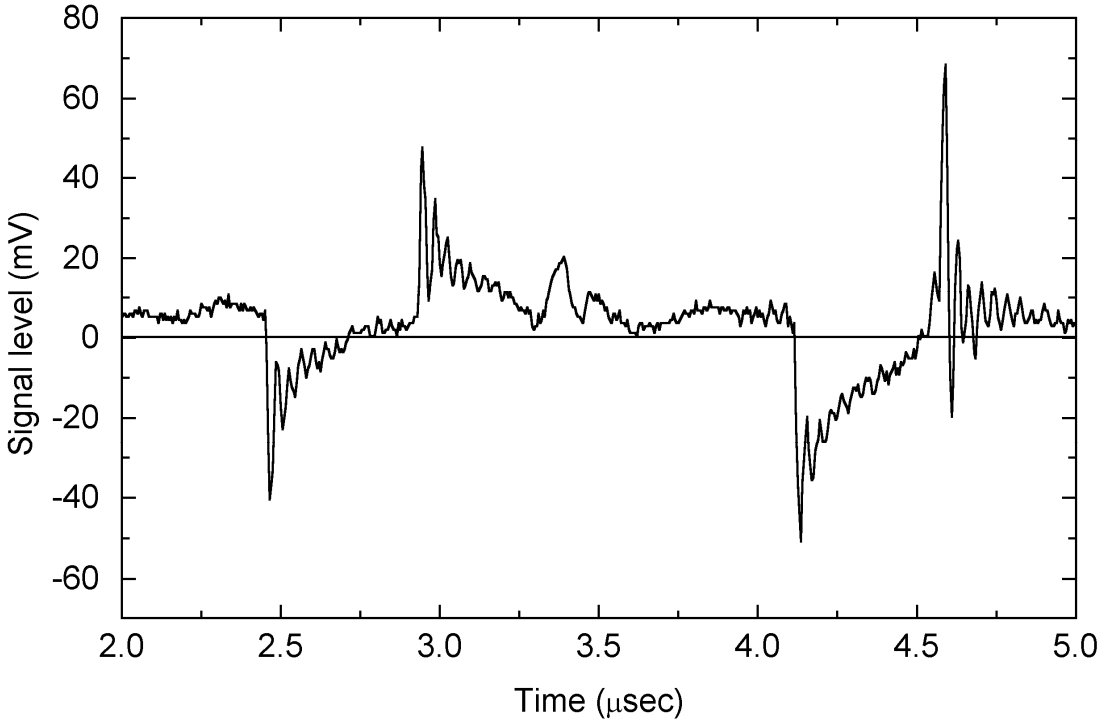
80
60
40
20
0
-20
-40
-60
Signal level (mV)
2.0
2.5
3.0
3.5
4.0
4.5
5.0
Time (μsec)

Figure 12.

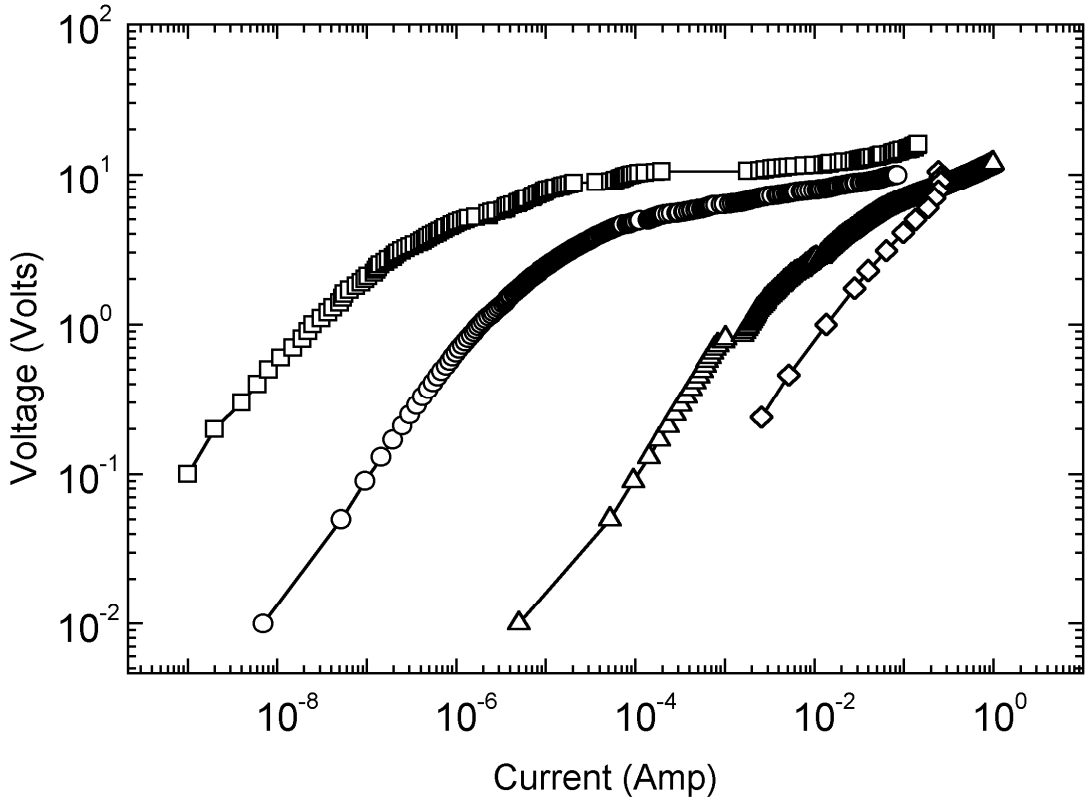
Voltage (Volts)
Current (Amp)
10^2
10^1
10^0
10^-1
10^-2
10^-8
10^-6
10^-4
10^-2
10^0

Figure 13.

(a)

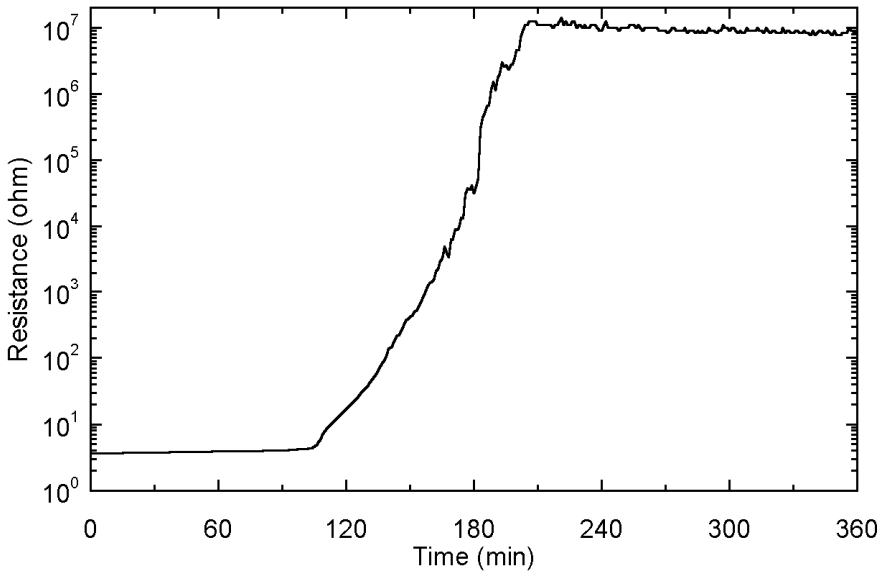
Resistance (ohm)
10^0
10^1
10^2
10^3
10^4
10^5
10^6
10^7
0
60
120
180
240
300
360
Time (min)

(b)

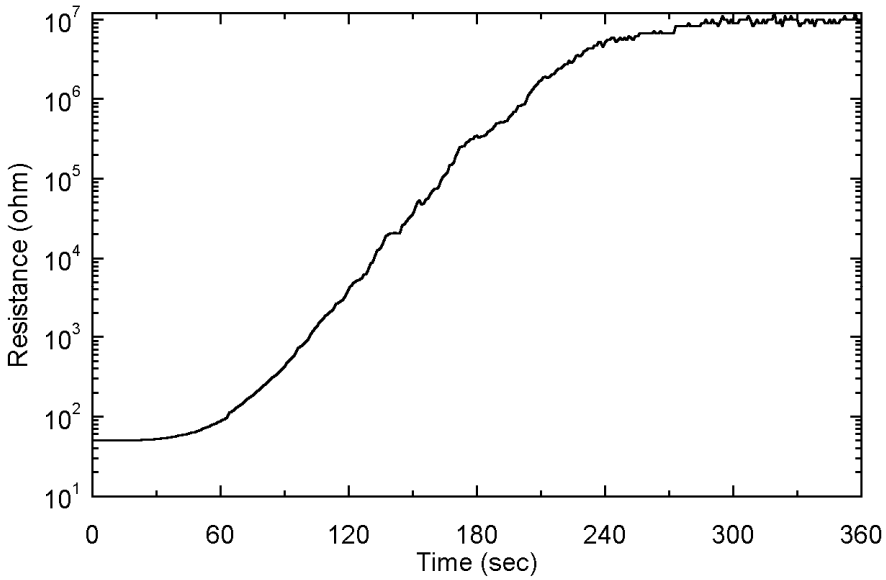
Resistance (ohm)
10^1
10^2
10^3
10^4
10^5
10^6
10^7
0
60
120
180
240
300
360
Time (sec)